PHYSICAL REVIEW C VOLUME 52, NUMBER 2 AUGUST 1995

Are there η-helium bound states?

S. Wycech*
Soltan Institute for Nuclear Studies, Warsaw, Poland

A.M. Green†
Research Institute for Theoretical Physics, P.O. Box 9, FIN-00014 University of Helsinki, Finland

J.A. Niskanen‡
Department of Physics, P.O. Box 9, FIN-00014 University of Helsinki, Finland
(Received 1 February 1995)

Using multiple scattering theory the scattering lengths of η mesons on helium nuclei are calculated and checked against final state η interactions from the $pd \to \eta^3$He and $dd \to \eta^4$He reactions. The existence of an η^4He quasibound state is indicated.

PACS number(s): 25.80.+e, 13.75.−n, 25.40.Ve

I. INTRODUCTION

In this paper we concentrate on the few-body interactions of η mesons. These could complement our knowledge on the η-nucleon interaction and give us possible evidence of η-nuclear quasibound states. Such quasibound states were predicted by Haider and Liu [1] and detailed calculations performed by Li *et al.* [2], when it turned out that the η-nucleon interaction was attractive. To be observable these states should be narrow enough, and this is not likely to happen for the lowest η states in large nuclei. On the other hand, it was suggested by Wilkin [3] that the rapid slope seen in the $pd \to \eta^3$He amplitude of Ref. [4] just above the threshold may signal that a quasibound state is generated already for small nuclei ($A = 3$). In contrast, a recent study of the $dd \to \eta^4$He reaction shows no structure due to any final state η^4He interaction [5]. All this could indicate a large η^3He scattering length and a small one for η^4He. However, quite an opposite interpretation is put forward in this paper. We calculate the η^3He and η^4He scattering lengths and find that the former is *smaller* than the latter, and that they also differ in the sign of the real part. This suggests that the η-nucleus attraction is not strong enough to give any binding effect in the η^3He system, but it is likely to give one in the η^4He system.

In the standard theory of final state interactions the energy dependence of reactions is assumed to be determined by the scattering amplitude between the final state particles [6]. In this paper we show that the shape of the low energy η production cross section is also significantly influenced by an interference of the free and scattered waves in the final η-helium states, because the corresponding scattering lengths are not very large. This interference is such that the decrease with energy becomes steeper for both ^{3}He and ^{4}He than that calculated from the final state scattering amplitude alone. However, in the scattering amplitude itself the real and imaginary parts of the scattering amplitude, due to the above mentioned difference in the sign of the real parts, could be expected to conspire so that the slope in the ^{4}He case would be somewhat smaller than for ^{3}He. Numerical results do not support this for ηN scattering lengths considered realistic.

Before this physical interpretation of final state interactions is discussed in Sec. III, a formalism is developed in Sec. II to calculate the η-helium scattering lengths. By some formal manipulations the multiple scattering series is summed. The procedure used is shown to converge quickly in the case of ηHe optical potentials, which may be solved exactly using the Schrödinger equation. Then, necessary corrections to the optical potential limit may be easily implemented by modifying the equivalent multiple scattering series.

The conclusions are not fully quantified since the η-nucleon input is not determined uniquely. Also the η production mechanism is not under full control. Here a method for calculating only the final state interaction is given. However, this method is presented in sufficient detail that a more complete comparison with the data and the determination of the input uncertainties can be made when measurements proposed at proton storage rings, such as the one at Celsius, are performed. Comparing specifically with the η^3He data we also perform an extensive variation of the ηN scattering length in search for a constraint on it, complementing elementary photoproduction or electroproduction.

II. SCATTERING LENGTHS

The η-helium scattering lengths are calculated in this section. At first we consider the simplest optical model

*Electronic address: wycech@fuw.edu.pl
†Electronic address: green@phcu.helsinki.fi
‡Electronic address: janiskanen@phcu.helsinki.fi

expressed in terms of the η-nucleon scattering length. This problem may be solved numerically, but in order to improve the method an equivalent alternative for the optical model is provided, which consists of a partial summation of the multiple scattering series generated by the optical potential. The sum is expressed in terms of multiple integrals.

Next, some necessary improvements to the optical model are introduced into the partial sum. These are essentially twofold: (i) removing multiple collisions on the same nucleon and (ii) introducing an off-shell η-nucleon scattering matrix. Other effects, e.g., the Pauli principle, are less significant. These improvements introduce massive changes to the η-helium scattering lengths defined here as the zero-energy limit of the effective range expansion

$$p \cot \delta = \frac{1}{a} + \frac{1}{2} r_0 p^2 . \quad (1)$$

In particular, for the η^3He system, the simplest optical model yields a large negative real part of the scattering length, indicating the existence of a quasibound state. However, when the corrections are included, a sizable positive scattering length emerges. On the other hand, in the η^4He system we do find indications for a quasibound state close to threshold.

A. Multiple scattering expansion for the inverse scattering length

In Ref. [7] a multiple scattering scheme was proposed to calculate the energy shifts and widths in the atomic states of antiprotons interacting with a light nucleus. In this paper we apply the same method to ηHe scattering at threshold. First the procedure is presented in some detail, since it is important to understand to what extent the basic form of the multiple scattering scheme is, in this case, numerically equivalent to the standard optical model approximation.

The scattering matrix $T(\eta A)$ for an η meson interacting with a nucleus of A nucleons may be expressed as a series in the following way by first considering the scattering from two nonoverlapping fixed centers. In that limit it can be shown that the scattering matrix at zero energy has the *exact* form [8]

$$T(\eta, 2) = \frac{T_1 + T_2}{1 - \frac{1}{2}\frac{(T_1+T_2)D(T_1+T_2)}{(T_1+T_2)}}, \quad (2)$$

where $D = 1/l$ is the propagator of the scattered particle, with l being the distance apart of the two scattering centers, and the T_i are the scattering matrices from the separate centers. This expression has the following feature that is important in few-body systems. By expanding the denominator, a multiple scattering series emerges which through the factor of 1/2 in the denominator automatically takes into account the exclusion of successive scatterings from the same center. Being guided by this and denoting $T = \sum T_i$, one might then naively expect an analogous expression for the scattering from A nonfixed centers to have the form

$$T(\eta A) = \langle T \rangle [1 + P]^{-1}, \quad (3)$$

where

$$P = -\frac{(A-1)\langle TDT \rangle}{A\langle T \rangle}, \quad (4)$$

with

$$D = -m/(2\pi|\mathbf{r} - \mathbf{r}'|) \quad (5)$$

the zero-energy propagator for a free η. Here m is the reduced mass of the ηA system. The factor $(A-1)/A$ generalizes the exclusion factor 1/2 in Eq. (2) in the following way. The averaged double scattering can be presented in terms of individual scatterings from different nucleons as

$$\langle TDT \rangle = \sum_{j \neq i} \sum_i \langle \psi_0 | T_j D T_i | \psi_0 \rangle . \quad (6)$$

The exclusion of successive scatterings on the same nucleon is effectively incorporated in the factor $(A-1)/A$, after which $\langle TDT \rangle$, etc., include total scattering amplitudes on all nucleons as in the optical potential, i.e., $T = \sum_i T_i$.

However, as it now stands Eq. (3) cannot be correct beyond $O(T^2)$, since it does not give the required form

$$\begin{aligned} T(\eta A) = \langle T \rangle &+ \left(\frac{A-1}{A}\right) \langle TDT \rangle \\ &+ \left(\frac{A-1}{A}\right)^2 \langle TDTDT \rangle \\ &+ \left(\frac{A-1}{A}\right)^3 \langle TDTDTDT \rangle + \cdots , \end{aligned} \quad (7)$$

when expanded in powers of T. One way of ensuring that this correct expansion results is to modify Eq. (3) to

$$T(\eta A) = \langle T \rangle [1 + P + Q + R + \cdots]^{-1}, \quad (8)$$

where the quantities $P, Q, R, \ldots$ are of order $T, T^2, T^3, \ldots$, respectively, and are chosen in turn to guarantee Eq. (7). For example, on expanding the denominator of Eq. (8) the term of $O(T^2)$ is $-Q + P^2$, which in Eq. (7) should give $\left(\frac{A-1}{A}\right)^2 \langle TDTDT \rangle$. Since P has already been fixed by the second term in Eq. (7), we get $Q = P^2 - \left(\frac{A-1}{A}\right)^2 \langle TDTDT \rangle$. This is a unique procedure and, neglecting for the moment the above exclusion of consecutive scatterings on the same nucleon, it leads to the expressions

$$\begin{aligned} P &= -\frac{\langle TDT \rangle}{\langle T \rangle}, \quad Q = \frac{\langle TDT \rangle^2}{\langle T \rangle^2} - \frac{\langle TDTDT \rangle}{\langle T \rangle}, \\ R &= -\frac{\langle TDT \rangle^3}{\langle T \rangle^3} + 2\frac{\langle TDTDT \rangle \langle TDT \rangle}{\langle T \rangle^2} \\ &\quad - \frac{\langle TDTDTDT \rangle}{\langle T \rangle}, \end{aligned} \quad (9)$$

for the first three terms of the series in the denominator. Also in $Q, R, \ldots$ it is immediately seen that the integers multiplying each term cancel each other; e.g., in Q we see +1 and −1, in R we see −1,+2,−1, etc. In the fixed center limit all of the integrals reduce to the same value, so that $Q, R, \ldots$ are then all zero as found in Ref. [8]. The important point is that numerically this cancellation continues to a great extent even away from the fixed center limit as seen below. Therefore, one could hope that the introduction of the ratios $\langle TDT\rangle/\langle T\rangle$, etc., of double and triple scatterings and other "disconnected" terms at various places would speed up the convergence of the multiple scattering series.

The multiple scattering expansion in Eq. (7) is a simple version of the Watson multiple scattering series applied to the case of identical scatterers [9]. In its full generality T is a sum of $t(i)$, the scattering matrices of the eta on the ith scatterer. The latter is the scattering matrix in the medium and it comes as a solution of the Lippman-Schwinger equation $t(i) = v(i) + v(i)Dt(i)$ with some potential $v(i)$ and a full propagator D for the eta-helium system. The same D describes the propagation between two successive collisions. In this paper we simplify the problem by using the free eta-nucleon scattering matrices in the low energy form $t(i) = -a/(1 - iKa)$, where a is the scattering length and K is the relative eta-nucleon momentum. It is justified by the short range of the eta-nucleon-N^* vertices involved in the interaction models [1,10], which are discussed briefly in the Appendix. In principle, one could expect medium effects in particular in the pion-nucleon decay channels. A brief estimate is given in the Appendix where we find these to be small. Another simplification involves the propagator D in the intermediate states between collisions. This we take as a projection on the helium ground state and a free propagation of the eta given by Eq. (5). With these simplifications we compare the summing of the multiple scattering series for two models: (1) optical potential, $t(i) = -a$ and $(A-1)/A \to 1$; (2) improved model, $t(i) = -a/(1 - iKa)$, where K involves binding plus recoil corrections along with the $(A-1)/A$ factors. While the first model is used to check the convergence of our summation, the second one is to discuss the physics of eta-helium scattering.

Here now T denotes a scattering matrix of the η from A nucleons in the impulse approximation. At "zero" energy $mT(\eta A)/2\pi$ reduces to minus the ηA scattering length $a(\eta A)$ and

$$T = \frac{2\pi}{\mu}\, t\, A\, \rho(r), \tag{10}$$

with t being the η-nucleon scattering matrix at the appropriate energy, $A\rho(r)$ the nuclear density, and μ the reduced mass for the ηN system. The expectation values appearing in Eqs. (9) can be expressed in terms of the propagator and nuclear density as

$$\langle T\rangle = \frac{2\pi}{\mu} tA \int d\mathbf{r}\, \rho(\mathbf{r}) = \frac{2\pi}{\mu}\, tA, \tag{11}$$

$$\langle TDT\rangle = -\frac{2\pi}{m}\left(\frac{m}{\mu}t\right)^2 A^2 \int\int d\mathbf{r}d\mathbf{r}'\, \rho(\mathbf{r})\frac{1}{|\mathbf{r}-\mathbf{r}'|}\rho(\mathbf{r}'), \tag{12}$$

$$\langle TDTDT\rangle = \frac{2\pi}{m}\left(\frac{m}{\mu}t\right)^3 A^3 \int\int\int d\mathbf{r}d\mathbf{r}'d\mathbf{r}''\, \frac{\rho(\mathbf{r})\rho(\mathbf{r}')\rho(\mathbf{r}'')}{|\mathbf{r}-\mathbf{r}'||\mathbf{r}'-\mathbf{r}''|}, \text{ etc.} \tag{13}$$

Using the Gaussian density profile

$$\rho(r) = [1/(\sqrt{\pi}R_0)^3] \exp[-(r/R_0)^2], \tag{14}$$

one obtains now the expansion coefficients

$$P = t\left(\frac{Am}{R_{\rm rms}\mu}\right)\sqrt{\frac{3}{\pi}}, \quad Q = t^2\left(\frac{Am}{R_{\rm rms}\mu}\right)^2\left[\frac{3}{\pi} - 1\right],$$

$$R = t^3\left(\frac{Am}{R_{\rm rms}\mu}\right)^3\left[\left(\frac{3}{\pi}\right)^{3/2} - 2\left(\frac{3}{\pi}\right)^{1/2} + 0.7796\sqrt{2}\left(\frac{3}{\pi}\right)^{3/2}\right], \tag{15}$$

where $R_{\rm rms} = \sqrt{3/2}R_0$ is the rms matter radius of the A nucleons. The number 0.7796 in R is the result of a double summation and is expected to have an accuracy of ± 0.0001. When the terms of the series in the denominator are clustered into increasing powers of t as indicated in Eqs. (8),(9), it is found that there exists a considerable amount of cancellation, e.g., $P/d = 0.977$, $Q/d^2 = -0.045$, and $R/d^3 = 0.0076$ where $d = t\,(Am/R_{\rm rms}\mu)$. Therefore, if $t/R_{\rm rms}$ is reasonably small — as it is in the present case of ηN scattering — the series appears to converge rapidly.

A check on the convergence is given in Table I, where a comparison is made between the above series expansion for $T(\eta A)$ and its value calculated directly from the equivalent optical model potential

$$V(\text{opt}) = \frac{2\pi}{\mu} tA\,\rho(r). \tag{16}$$

In this comparison the factors $(A-1)/A$ in Eq. (7) must be neglected. For completeness, the impulse approximation (IA) result

$$a(\eta A, \text{IA}) = -A\,\frac{m}{\mu}\,t \tag{17}$$

is also quoted in Table I [i.e., $T(\eta A)$ with $P = Q = R = 0$]. As a first approximation t is taken to be minus the ηN scattering length, i.e., $t(E=0) = -a(\eta N)$. The actual numbers used are a representative sample from the following sources. Several groups have performed coupled channel analyses of η-nucleon and π-nucleon scattering [1–3,10,12,13]. These differ in the input data and also in some details of the extraction of the $a(\eta N)$. The ηN scattering lengths obtained are $0.27 + i0.22$ and $0.28 + i0.19$ [12] and $(0.50 \pm 0.20) + i(0.33 \pm 0.06)$ fm [3]. The recent electroproduction data yield $0.476 + i0.279$ fm [10], while photoproduction experiments suggest the possibilities $0.430 + i0.394$, $0.579 + i0.399$, $0.291 + i0.360$ fm [13].

The multiple scattering effect is dramatic as compared with the impulse approximation alone, changing the attractive real part of the ηN amplitude into a repulsive real part for the ηA amplitude. However, the near equality between $a(\eta A)$ and $a(\text{opt})$ gives confidence that, indeed, the series in Eq. (8) is rapidly convergent and the use of only the terms P, Q, and R gives a sufficient accuracy.

Having shown in some detail that, indeed, the standard optical model approach can be replaced by the multiple scattering series of Eq. (8), it now seems justified to modify the latter to include effects not so easily incorporated directly into the optical model.

B. Corrections to the optical model

Several improvements can be made to the optical model approach and these can be implemented into the partial sum of Eq. (8).

(i) First, as shown in Eq. (7) the factors $A^{1,2,3}$ in the rescattering quantities P, Q, and R calculated in Eqs. (15) should be replaced by $(A-1)^{1,2,3}$ to prevent the η from interacting successively with the same nucleon, i.e., $a(\eta A) \to a_{A-1}(\eta A)$. In Table II this effect is demonstrated for the ηN scattering lengths used in Table I, and it is seen to have a large effect in all cases. In particular, this correction makes the real parts of the scattering lengths small for ^{3}He, making the existence of a quasibound state in the η^3He system indicated by the optical model questionable. The absence of such a state seems to be further confirmed by later corrections for ^{3}He. However, the real parts tend to become even more negative in the case of ^{4}He.

(ii) Another improvement to the above series is to use an ηN scattering amplitude that is more appropriate for scattering on a bound nucleon in a medium. This can be approximately taken into account by extrapolating $a(\eta N)$ off the energy shell through replacing the above scattering amplitude $a(0)$ at zero energy by $a(\text{off})$ at a negative energy defined via the equation

$$\frac{1}{a(0)} \to \frac{1}{a(\text{off})} = \frac{1}{a(0)} - iK_\eta, \tag{18}$$

where $K_\eta = i\sqrt{2\mu(E_{\rm sep} + E_{\rm rec})}$ with $E_{\rm sep,rec}$ being the $A \to (A-1) + 1$ separation energy and the recoil energy of the ηN pair relative to the residual nucleus. For ^{3}He (^{4}He) these quantities have the values $E_{\rm sep} = 7$ (21) MeV and $E_{\rm rec} = 12$ (12) MeV. The effects are shown

TABLE I. Comparison for η-He scattering lengths $a(\eta\text{He})$ (in fm) from various stages of the series expansion in Eq. (8) with the results from direct calculation with the corresponding optical potential [11]. The numbers are for ^{3}He and those in the brackets refer to ^{4}He. The results are illustrated with four sets of the ηN input: $a(\eta N) = 0.476 + i\,0.279$ fm (I), $0.579 + i\,0.399$ fm (II), $0.430 + i\,0.394$ fm (III), and $0.291 + i\,0.360$ fm (IV). In all cases $R_{\rm rms} = 1.788\,[1.618]$ fm.

$a(\eta N)$	$a(\text{IA})$	$Q=R=0$	$R=0$	$a(\eta A)$	$a(\text{opt})$
I	$1.89 + i1.11$	$-2.00 + i3.01$	$-1.94 + i2.65$	$-1.89 + i2.60$	$-1.87 + i2.59$
	$[2.63 + i1.54]$	$[-2.46 + i1.27]$	$[-2.14 + i1.12]$	$[-2.05 + i1.13]$	$[-2.01 + i1.16]$
II	$2.30 + i1.59$	$-2.41 + i1.94$	$-2.16 + i1.71$	$-2.08 + i1.70$	$-2.06 + i1.72$
	$[3.20 + i2.20]$	$[-2.24 + i0.83]$	$[-1.91 + i0.79]$	$[-1.81 + i0.83]$	$[-1.79 + i0.90]$
III	$1.71 + i1.57$	$-1.67 + i2.12$	$-1.56 + i1.93$	$-1.52 + i1.92$	$-1.51 + i1.93$
	$[2.38 + i2.18]$	$[-2.03 + i1.13]$	$[-1.78 + i1.06]$	$[-1.70 + i1.08]$	$[-1.70 + i1.12]$
IV	$1.16 + i1.43$	$-0.93 + i1.92$	$-0.90 + i1.81$	$-0.89 + i1.80$	$-0.88 + i1.80$
	$[1.61 + i1.99]$	$[-1.62 + i1.38]$	$[-1.47 + i1.28]$	$[-1.42 + i1.30]$	$[-1.42 + i1.31]$

TABLE II. The notation is the same as Table I except that the A^n, factors in P, Q, and R are now replaced by $(A-1)^n$, giving $a_{A-1}(\eta A)$ as indicated by Eq. (7).

$a(\eta N)$	$Q' = R' = 0$	$R' = 0$	$a_{A-1}(\eta A)$	$a(\text{opt})$
I	0.53+i4.27	0.30+i4.19	0.28+i4.16	−1.87+i2.59
	[−3.01+i2.94]	[−2.76+i2.55]	[−2.67+i2.51]	[−2.01+i1.16]
II	−1.52+i4.40	−1.61+i4.06	−1.59+i4.01	−2.06+i1.72
	[−3.03+i1.84]	[−2.67+i1.64]	[−2.56+i1.65]	[−1.79+i0.90]
III	−0.53+i3.35	−0.61+i3.21	−0.60+i3.18	−1.51+i1.93
	[−2.38+i2.23]	[−2.16+i2.02]	[−2.09+i2.02]	[−1.70+i1.12]
IV	−0.13+i2.36	−0.16+i2.31	−0.16+i2.30	−0.88+i1.80
	[−1.53+i2.25]	[−1.45+i2.10]	[−1.41+i2.09]	[−1.42+i1.31]

in Table III. There it is seen that our best estimate $a_{A-1}(\eta A, \text{off})$ of the ηA scattering length is quite different from that predicted by the optical model. For example, in η^3He scattering, the negative Re a(opt) has turned positive and comparable to that of the original impulse approximation. This indicates that there is no binding in this system. However, for η^4He the negative sign of Re a(opt) is maintained, suggesting a quasibound state. At the end of this section these effects are interpreted in terms of poles in the scattering matrix. One should note in this context that, since in Eq. (18) a significant nonzero value is assigned for the η momentum, the next term in the effective range expansion (1) could become important if r_0 is large. This could have now the effect of changing the energy variation present in Eq. (18).

(iii) The major mechanism that generates the imaginary part of $a(\eta A)$ is the reaction $\eta A_i \to N^*(A-1) \to \pi A_f$, where N^* is the nucleon resonance $N^*(1535)$ with a strong coupling to both the η and the pion. Therefore, for η scattering on deuterium or ^{4}He—both isoscalars—the final nucleus A_f cannot be an isoscalar. Because the spin is not involved in this s-wave scattering, then, for example, with the deuteron the final NN state must be the $^3P_1$ state and also the transition operator must be spatially antisymmetric. This opens up the interesting possibility that pionic inelastic channels are damped in these cases, leading to a reduction of the in-medium value of Im $a(\eta N)$. However, as shown in the Appendix this turns out to be only a very small effect and so this correction is not included in the present calculations.

In the situation of a single channel scattering and a weak attractive force a positive scattering length is generated. An increasing attraction makes the length grow until one meets the first critical point as $a \to \infty$. This point signals a bound state at zero energy. When the binding is made stronger but a second bound state (the second critical point) is not yet reached the scattering length stays negative. The sum in Eq. (8) converges quickly in some region well below the critical point. Now, even if there is no bound state on a nucleon, there might be a bound state on a nucleus and such situations are well handled by Eq. (8) at least around the first nuclear bound state. A negative $a(\eta, A)$ would signal a bound state. The weak attraction is approximately the situation encountered in the eta-nucleon case, but a more realistic description requires addition of the pion-nucleon channel. Here some caution is necessary, since the latter may reduce or enhance the attraction and induce an absorptive part into the effective eta-nucleon potential and scattering length Im a. Also there is two-nucleon absorption present [14]. In such a situation the relation between the sign of Re a and the sign of the real part of the effective eta-nucleon potential becomes more involved. In particular, even a mildly attractive potential may generate a repulsive (negative) length. This is known as the repulsive effect of the absorption and similar effects are expected for the bound state energy and width [15]. On the other hand, if there is only one bound state, its existence is still correlated with the sign of the Re a provided Re a is large and the effective range is small or comparable to the force radius. Such a situation is not met in the eta-nucleon case, but to some extent the condition is fulfilled in the eta-helium cases.

If there exists a pole in the scattering matrix close to

TABLE III. The notation is the same as in Table II except that $a(\eta N)$ is now calculated off-shell using $E_{\text{sep}} + E_{\text{rec}} = 19$ (33) MeV corresponding to $iK_\eta = 0.581$ (0.766) fm^{-1}.

$a(\eta N, 0)$	$a(\eta N, \text{off})$	$R' = 0$	$a_{A-1}(\eta A, \text{off})$	$a_{A-1}(\eta A, 0)$
I	0.39+i0.17	2.01+i2.85	1.99+i2.86	0.28+i4.16
	[0.37+i0.15]	[−1.56+i5.30]	[−1.59+i5.19]	[−2.67+i2.51]
II	0.47+i0.22	1.36+i4.38	1.32+i4.37	−1.59+i4.01
	[0.44+i0.18]	[−3.14+i3.88]	[−3.07+i3.77]	[−2.56+i1.65]
III	0.39+i0.24	0.93+i3.08	0.92+i3.07	−0.60+i3.18
	[0.37+i0.21]	[−1.76+i3.69]	[−1.73+i3.62]	[−2.09+i2.02]
IV	0.29+i0.26	0.59+i2.17	0.58+i2.17	−0.16+i2.30
	[0.29+i0.23]	[−0.78+i2.95]	[−0.78+i2.93]	[−1.41+i2.09]

the threshold, the scattering lengths may become larger than the nuclear radius. To some extent this situation is met here, in particular in ^{4}He. In the case of a bound state Re $a < 0$, while a virtual state corresponds to Re $a > 0$. The connection is unique provided the effective range is small, which is assumed here. However, the validity of this assumption is not clear. Another complication arises because of the presence of decay channels described here by Im $a(\eta N)$. Even though there is no detailed many-channel structure of the scattering matrix, let us, however, look for the poles given by the condition $(1 - ipa)= 0$. With our best values $a_{A-1}(\eta A, \text{off})$ we have a pole in the upper complex momentum half plane, i.e., a quasibound state in the η^4He case. This situation is, in fact, typical for all Re $a(\eta N)$ in the range 0.3–0.6 fm or even higher. On the other hand, with positive Re $a_{A-1}(\eta A, \text{off})$ one meets a virtual state in η^3He systems.

III. FINAL STATE INTERACTIONS

Since there are no beams of η mesons, the interactions of these mesons may be seen only via final state interactions or via the decay mechanisms of quasibound states. As seen in Fig. 1, the $pd \to \eta^3$He production amplitude displays a rapid falloff away from the threshold region, which led Wilkin to conjecture that an η^3He quasibound or resonance state exists nearby [3]. This is reflected by the approximate proportionality of the cross section to the final state interaction factor [6]

$$|F_1|^2 = \left| \frac{a(\eta A)}{1 - ipa(\eta A)} \right|^2 , \quad (19)$$

where $a(\eta A)$ is the η-helium scattering length and p is the η momentum. It was found by Wilkin in the optical potential approach [3], recalculated here in Sec. II, that Im $a(\eta^3\text{He})$ is rather large, which gives the required slope and indicates a singularity. However, surprisingly the recent data on the reaction $dd \to \eta^4$He indicate no such slope in the cross section close to the threshold [5]. We now analyze these two measurements below.

First, let us note that Eq. (19) provides a good description only if $|a(\eta A)| \gg R_{\text{rms}}$, a condition not well satisfied here by the R_{rms} for ^{3}He. A more general model needs the final s-state wave function for the η-He system $\psi^-(r)$. One particularly simple form of $\psi^-(r)$ is that from a separable potential with the Yamaguchi form factors $(1 + p^2/\beta^2)$ [17], which gives

$$\psi^-(r) = \frac{\sin(pr)}{pr} + f^* \frac{[\exp(-ipr) - \exp(-\beta r)]}{r} . \quad (20)$$

Here $f = F_1 = a(\eta A)/[1 - ipa(\eta A)]$ is the on-shell η-helium scattering matrix, where the $a(\eta A)$ are taken to be the $a_{A-1}(\eta A, \text{off})$ from Sec. II and not the $a(\eta A)$ given by the separable potential. Since the factor $[\exp(-ipr) - \exp(-\beta r)]$ determines the behavior of the scattered wave inside the range of the interaction, it can be interpreted as producing an off-shell effect into the reaction. A plausible choice of $\beta = 1/R_{\text{rms}}$ is taken, but, as shown below, the shape of the cross section is rather insensitive to the actual value of β.

In the reaction process the η's are produced with some amplitude $H(r, p_i)$ that depends both on the initial projectile momentum (p_i) and on the spatial extent of the process. For η energies in the range of 0–5 MeV the dependence on p_i ($\approx$1 GeV) is presumably small. So far there is no complete understanding of the actual production mechanism [3,18]. However, for the present purposes it is sufficient to make only some rather general qualitative statements concerning this mechanism. Here we simply assume a proportionality of the production am-

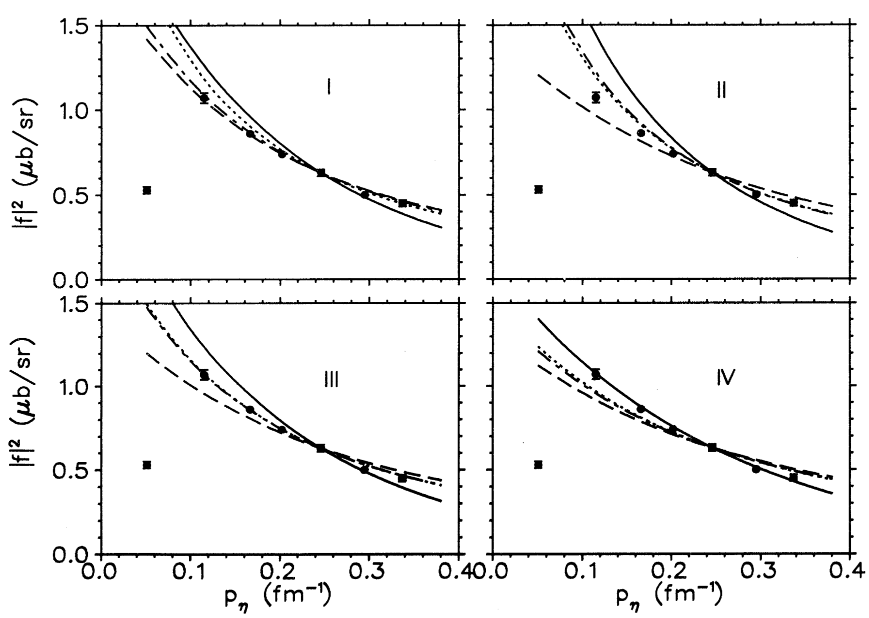

FIG. 1. The $pd \to \eta^3$He amplitude square $|f(\text{expt})|^2$ defined in Eq. (22) plotted against the η momentum in the c.m. system for the four elementary ηN amplitudes I–IV given in Table I. Dashed curve, optical model; dotted curve, optical model corrected by $A \to A-1$ but described by Eq. (19); dash-dotted curve, off-shell effect also included in Eq. (19); solid curve, the full model with corrections to the optical model and with the background term in the wave function (20). The data are from Refs. [3,4,16].

plitude to the nuclear density used to derive Eq. (15), $H(r) = \exp\left[-(r/R_0)^2\right]$, with $R_0 = \lambda\sqrt{2/3}R_{\rm rms}$ and $\lambda \approx 1$ being a natural choice. In this way, the final state interaction factor becomes

$$|F_2(\lambda,\beta)|^2 = \left|\int \bar{\psi}^-(r)\ H(r)d\bar{r}\right|^2. \qquad (21)$$

The difference between F_1 and F_2 is from the unscattered background term in Eq. (20).

At first sight it appears that this model for incorporating final state interactions contains two adjustable parameters λ and β. However, in practice the β dependence is weak with even $\beta = \infty$ being not unreasonable. As said above, we typically fix β at $1/R_{\rm rms}$, leaving only the λ dependence. Lacking an actual model for η production, in all cases the results are normalized to give the experimental value of the spin-averaged quantity

$$|f(\text{expt})|^2 = \frac{p_d}{p_\eta}\frac{d\sigma}{d\Omega}(pd \to \eta^3\text{He}) = 0.63 \pm 0.02\ \mu\text{b/sr} \qquad (22)$$

at $p_\eta = 0.246\ \text{fm}^{-1}$.

The original hope had been that, with λ around unity, a good fit would be obtained to the shape of the experimental data. However, this was only so for potential IV. In that case, with λ=0.88 and $\beta = 1/R_{\rm rms}$ there was a very shallow minimum in the χ^2 fit to $|f(\text{expt})|^2$. It should be added that this fit did not include the lowest experimental point at $p_\eta = 0.051\ \text{fm}^{-1}$, since this is thought to be subject to large systematic errors due to beam width effects, including energy losses in the target [3]. The results are shown in Table IV and Fig. 1.

Table IV illustrates the following points:

(1) As seen from columns 3 and 4 the dependence on β is weak. Both $\beta = 1/R_{\rm rms}$ and ∞ yield good fits to the data, since fixing $\beta = 1/R_{\rm rms}$ gives χ^2/data point (dp) = 0.35, which is increased to only 1.02 for $\beta = \infty$.

(2) In column 5 the use of only $|F_1|^2$ as in Ref. [3] is clearly inferior with its $\chi^2/\text{dp} = 6.63$.

(3) The normalization factors needed to fit the experimental value of 0.63 μb/sr at $p_\eta = 0.246\ \text{fm}^{-1}$ are 0.87, 0.31, 1.50 for columns 3, 4, 5, respectively. This shows that $|F_2|^2$ is 1.7 times stronger than $|F_1|^2$ and so could account for a significant part of the factor of 2.5 by which the model of Ref. [19] underestimated the experimental data.

It should be added that there is a strong correlation between λ and β; e.g., for $\beta = 2/R_{\rm rms}$ the minimum χ^2/dp is still 0.35 but with λ=0.97. The dependence on the parameter λ is also weak as it is with β. Therefore, the main dependence may be expected to arise from the input values of the elementary ηN scattering amplitude.

Unfortunately, the refinement in going from $|F_1|^2$ to $|F_2|^2$ gives fewer benefits with the other potential options.

(a) For potential III, with $\beta = \infty$, a χ^2/dp minimum of 0.58 occurs at $\lambda = 0.38$ to be compared with χ^2/dp=0.71 for $|F_1|^2$; i.e., little is gained by the refinement, in both cases a good fit being achieved to the data. Again there is a strong correlation between λ and β with the above χ^2/dp=0.58 arising also for $\beta = 1/R_{\rm rms}$ and $\lambda = 0.14$.

(b) Potential I gives already a good fit to the data using $|F_1|^2$ with χ^2/dp=0.61. This cannot be matched by $|F_2|^2$, which gives χ^2/dp=16 with $\beta = 1/R_{\rm rms}$ and $\lambda = 1$. This only improves as β increases and λ decreases, i.e., finally back to $|F_1|^2$.

(c) Potential II is the worst combination. Here $|F_1|^2$ gives χ^2/dp=6.5. In comparison $|F_2|^2$ using $\beta = 1/R_{\rm rms}$ and $\lambda = 1$ gives χ^2/dp=49; i.e., neither model gives a reasonable fit to the data. As with potential I, this only improves as the $|F_1|^2$ limit is approached.

The corresponding results with potential IV for ^{4}He are shown in Fig. 2. There it is seen that $|F_1|^2$ from Eq. (19) gives a visually better fit to the data and that $|F_2(\lambda = 0.88, \beta = 1/R_{\rm rms})|^2$ appears to produce too much energy dependence. However, it should be noted that here the experimental data have large error bars and exist only at a few energies. In the opinion of the authors, this should not be considered a fatal problem. Clearly some reduction of the experimental errors would be welcome to make these data more selective.

So far the values of $a(\eta N)$ used are those suggested by experiment. However, these differ considerably among themselves with $a(\eta N)$=[0.3–0.6]+i[0.3–0.4] fm being a more reasonable estimate (see caption of Table I). In

TABLE IV. The final state interaction factors $|F_i(\lambda,\beta)|^2$ in units of μb/sr for the elementary amplitude IV [$a(\eta N) = 0.291 + i0.394$], with $\lambda = 0.88$ and $\beta = 1/R_{\rm rms}$ or ∞.

p_η	$\lvert f(\text{expt})\rvert^2$	$\lvert F_2\rvert^2$	$\lvert F_2(\beta=\infty)\rvert^2$	$\lvert F_1\rvert^2$
0.051	0.53(0.02)	1.37	1.32	1.21
0.115	1.07(0.03)	1.06	1.02	0.95
0.166	0.86(0.015)	0.86	0.84	0.80
0.202	0.74(0.014)	0.75	0.74	0.72
0.246	0.63(0.020)	0.63	0.63	0.63
0.295	0.50(0.016)	0.52	0.53	0.55
0.337	0.45(0.018)	0.44	0.46	0.49

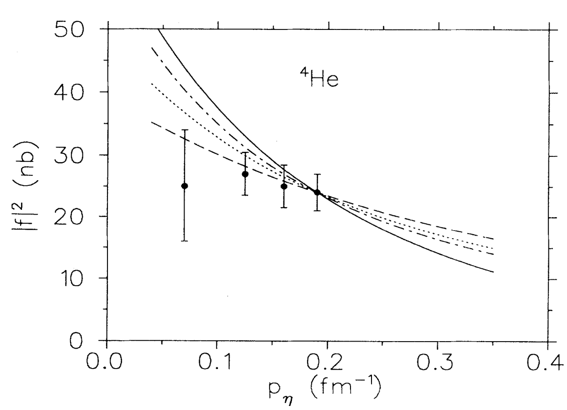

FIG. 2. The $dd \to \eta^4$He amplitude squared for the elementary ηN amplitude IV. Dots, data from [5] (normalized as the total cross section). Curves as in Fig. 1.

view of this, it is of interest to make a global variation of the input $a(\eta N)$ to recognize the optimal regions to fit the $pd \rightarrow \eta^3$He cross section data within different model regimes. Such a calculation was performed for $\beta = 1/R_{\rm rms}$ and $\lambda = 1$, i.e., in a crude model where these are not varied. Figure 3 shows the results for $\sqrt{\chi^2/\mathrm{dp}}$ in the complex $a(\eta N)$ plane. In the hatched regions this parameter is smaller than unity and other contours show the values 2,3,...,10. It can be seen that there is a systematic change due to each correction introduced in this work into the optical model results, with all these additional effects being in the same direction. There may be a common area around $a(\eta N) = 0.4 + i0.3$ fm for the optical model [3] without a Born background introduced in Eq. (20) and for the full model, but elsewhere the models are exclusive. The ^{3}He data would allow in each model a valley of minimum χ^2 in different regions for $a(\eta N)$. So it is clear that (even assuming that the production mechanism were known) these data cannot uniquely determine the scattering length, although they set a strong constraint. It may be noted that similar fits could be attempted for the ^{4}He data. However, there the quoted experimental errors are so large that as such the fit would be useless. Even so, the energy independence of the production amplitude indicated by the four existing data points close to the $dd \rightarrow \eta^4$He threshold is very suggestive. It was not possible to produce this feature with any reasonable value of the elementary scattering lengths allowed by the above considered models for ^{3}He. Similar energy dependences in the ^{4}He case are also obtained by Wilkin in Ref. [20].

IV. CONCLUSIONS

This paper is in two distinct parts. In the first, the basic η-nucleon scattering length $a(\eta N)$ is converted into effective η-^{3,4}He scattering lengths $a(\eta^{3,4}\mathrm{He})$, which, in the second part, are then used to calculate the final state interactions in the $pd \rightarrow \eta^3$He and $dd \rightarrow \eta^4$He reactions.

The step from $a(\eta N)$ to $a(\eta^{3,4}\mathrm{He})$ is made in two stages, applying a multiple scattering expansion and using free ηN scattering as a starting point. The accuracy of this procedure was first checked in the optical model limit, a limit that could be calculated directly from the Schrödinger equation (see Table I). Both the first stage, in which the replacement $A \rightarrow (A-1)$ is made, and the second stage, in which the scattering from a nucleon that is bound is taken into account, give large corrections that tend to go in the same direction. The overall effect is to give $a(\eta^{3,4}\mathrm{He})$'s that are very different from those expected using the pure optical model (see Tables II and III). However, it should be added that this calculation ignores the effect of the possible presence of a sizable effective range in the basic ηN interaction.

When the above $a(\eta^{3,4}\mathrm{He})$'s are used to extract the effect of final state interactions from the $pd \rightarrow \eta^3$He reaction, it is found that only one (option IV) of the $a(\eta N)$'s proposed in the caption of Table I is able to give a good fit to the ^{3}He data, but not the less restrictive ^{4}He data (see Figs. 1 and 2).

In an attempt to see if there exist other values of $a(\eta N)$ that can give a good fit to ^{3}He and, in addition, give a better fit to the ^{4}He data, a search was made in the region $1.0 \geq \mathrm{Re}\, a(\eta N) \geq -1.0$ and $1.0 \geq \mathrm{Im}\, a(\eta N) \geq 0.0$. However, this did not produce any $a(\eta N)$ significantly better than the earlier option IV. If one may disregard the ^{4}He data either as too inaccurate or arising from too complex a reaction, it seems that the ^{3}He results indicate some potential for constraining the elementary ηN scattering length.

ACKNOWLEDGMENTS

This paper follows the initiative of Torleif Ericson to study the theory and phenomenology of η physics around Celsius. The authors wish to thank Colin Wilkin very much for kindly supplying optical model results. One of us (S.W.) wishes to thank the Research Institute for Theoretical Physics in Helsinki, where most of this work was carried out, and also the Swedish Institute for supporting his earlier stay in Uppsala. J.A.N. was partly supported by the Academy of Finland.

APPENDIX: ISOSPIN 0 STATES

The η-deuteron and η-^{4}He systems are special cases. These are isospin 0 systems. Therefore, some decay modes to the pion-nucleon channels are not allowed by isospin conservation. In the multiple scattering expansion this blocking is due to a cancellation of pionic waves emitted from several coherent sources. This effect has been shown to be important in coherent η-production processes [21].

Here we first summarize briefly a two-channel description of η-nucleon scattering. Then we discuss the question of blocking the pionic channel in isospin 0 systems. We follow the standard description [1,10] in terms of a separable matrix $\hat{T}$ or $\hat{V}$ dominated by coupling to the $N^*(1535)$ resonance. Let $\hat{V}$ be

$$V_{ij} = \frac{f_i f_j}{E - M_0}, \tag{A1}$$

where M_0 is the bare mass of the N^* and the f_i are couplings to the different channels. The latter are functions of the channel momenta q_η and q_π. The scattering matrix $\hat{T}$ follows from the Lippman-Schwinger equation

$$\hat{T} = \hat{V} + \hat{V}(E - H_0 + i\epsilon)^{-1}\hat{T}. \tag{A2}$$

The separability of the interaction (A1) then allows for the simple solution

$$T_{ij} = \frac{f_i f_j}{E - M_0 - \sum_k \langle G_k \rangle}, \tag{A3}$$

where

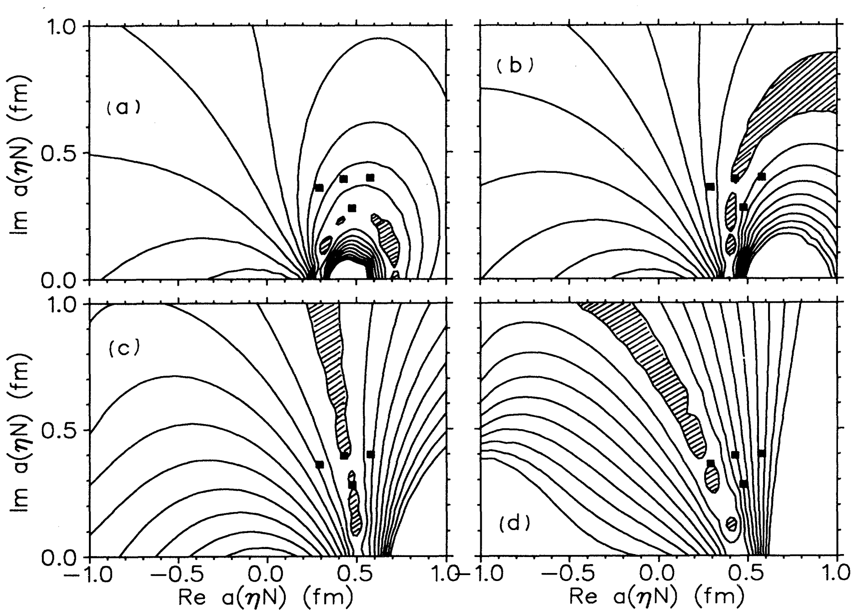

FIG. 3. Contour diagrams of $\sqrt{\chi^2/\mathrm{dp}}$ for different models: (a) optical model, (b) optical model corrected by $A \to A-1$ but described by Eq. (19), (c) off-shell effect also included, and (d) the full model with corrections to the optical model and with the background term in the wave function (20).

$$\langle G_k \rangle = \int \frac{d\mathbf{q}}{(2\pi)^2} N(q) \frac{f_k^2(q)}{E - E_k(q)}. \tag{A4}$$

The value of the total Re $\langle G \rangle$ yields an energy shift for the N^*, while Im $\langle G \rangle$ determines its width. With a relativistically invariant normalization $N(q)$ for both the η and N in Eq. (A4) one obtains, for the partial width into channel k,

$$\frac{\Gamma_k}{2} = -\mathrm{Im}\,\langle G_k \rangle = \frac{q_k(E)\, M_N\, f_k^2(q_k(E))}{4\pi E} \tag{A5}$$

and $T_{\eta\eta}(0) = -a(\eta N)$. The parameters of the coupling strengths and form factor ranges may be fitted to η-photoproduction (electroproduction) and π-nucleon scattering data as well as to the N^* decay properties. Analyses of this sort have been performed by several groups [1,10,22]. These differ slightly in the treatment of relativistic effects and on the (uncertain) input, and there is significant variation in the actual predictions for the scattering lengths $a(\eta N)$.

Now, let us consider η scattering on a correlated $S=1$, $T=0$ pair of nucleons forming a quasideuteron state. The intermediate states in the pionic channels have $T=1$ and so, due to the Pauli principle, the intermediate nucleons must be antisymmetric in space coordinates. This may reduce the available phase space and so lead to a blocking of virtual (or real) η-π transitions. As a consequence, the effective Im $a(\eta N)$ may be reduced in a nuclear medium. To allow for this effect we calculate the correction to the $\langle G_\pi \rangle$ of Eq. (A4) due to this Pauli effect. An average quantity

$$\frac{1}{4}\langle (f_1+f_2) G_{\pi NN} (f_1+f_2) \rangle \tag{A6}$$

is calculated with an antisymmetrized free NN propagator, the average being taken over the NN ground state. Further, in this estimate a zero-range interaction is assumed between the meson and nucleons, which are considered to be fixed. In this way a correction term $\langle \Delta G_\pi \rangle$ is obtained in the form

$$\langle \Delta G_\pi \rangle = \int \frac{d\mathbf{q}_\pi}{(2\pi)^3} N(q_\pi) \frac{f_\pi^2(q_\pi)\Delta(q_\pi)}{E - E_\pi(q_\pi)}, \tag{A7}$$

where

$$\Delta(q) = \int d\mathbf{u}\phi_{NN}^2(\mathbf{u}) \left[2\sin^2\left(\frac{\mathbf{q}\cdot\mathbf{u}}{2}\right) - 1\right] = -\tilde{\rho}(\mathbf{q}). \tag{A8}$$

Here ϕ_{NN} is the initial NN wave function and $\tilde{\rho}$ is the Fourier transform of the related density. For large systems this correction disappears, since $\langle 2\sin^2(\frac{\mathbf{q}\cdot\mathbf{u}}{2})\rangle \to 1$. But it could be sizable, if the inverse R_{rms} of the system is comparable to the momenta involved. However, for Im $\langle \Delta G_\pi \rangle \propto q_\pi \tilde{\rho}(q_\pi) f_\pi^2(q_\pi)$ with $q_\pi \approx 2$ fm^{-1} one finds only a few percent change of the N^* width in the deuteron and in helium. This is so small a correction — also obtained at high momentum, where the wave functions tend to be uncertain — that it is reasonable to neglect its effect.

[1] Q. Haider and L.C. Liu, Phys. Lett. B **172**, 257 (1986); Phys. Rev. C **34**, 1845 (1986).

[2] G.L. Li, W.K. Cheung, and T.T.S. Kuo, Phys. Lett. B **195**, 515 (1987).

[3] C. Wilkin, Phys. Rev. C **47**, R938 (1993).

[4] M. Garcon *et al.*, in *Proceedings of the Workshop on Spin and Symmetry in the Standard Model*, Lake Louise, Alberta, 1992, edited by B.A. Campbell (World Scientific,

Singapore, 1993).
[5] R. Frascaria *et al.*, Phys. Rev. C **50**, R537 (1994).
[6] K.M. Watson, Phys. Rev. **88**, 1163 (1952).
[7] S. Wycech and A.M. Green, Z. Phys. A **344**, 117 (1992).
[8] L.L. Foldy and J.D. Walecka, Ann. Phys. (N.Y.) **54**, 447 (1969).
[9] M.L. Goldberger and K.M. Watson, *Collision Theory* (John Wiley and Sons, New York, 1964), Chap. 11, Sec. 3.
[10] L. Tiator, in *Proceedings of the II TAPS Workshop*, Guadamar, 1993, edited by J. Diaz and Y. Schutz (World Scientific, Singapore, 1994); Mainz Report No. MKPH-T-93-16, 1993; L. Tiator, C. Bennhold, and S. Kamalov, Nucl. Phys. **A580**, 455 (1994).
[11] C. Wilkin (private communication).
[12] R.S. Bhalerao and L.C. Liu, Phys. Rev. Lett. **54**, 865 (1985).
[13] B. Krusche, in *Proceedings of the II TAPS Workshop* [10].
[14] H.C. Chiang, E. Oset, and L.C. Liu, Phys. Rev. C **44**, 738 (1991).
[15] R.H. Landau and J. Schnick, Phys. Rev. C **36**, 1942 (1987).
[16] B. Nefkens (private communication); R. Kessler, Ph.D. thesis, UCLA, 1992.
[17] Y. Yamaguchi, Phys. Rev. **95**, 1628 (1954).
[18] J.M. Laget and J.F. Lecolley, Phys. Rev. Lett. **61**, 2069 (1988).
[19] G. Fäldt and C. Wilkin, Uppsala University Report No. TSL/ISV-94-105, 1994.
[20] C. Wilkin, Phys. Lett. B **331**, 276 (1994).
[21] B. Lopez Alvaredo and E. Oset, Phys. Lett. B **324**, 125 (1994).
[22] C. Bennhold and H. Tanabe, Nucl. Phys. **A530**, 625 (1991).